

Visualization of Fiber Moving in Air Tunnel with Velocity Gradient *

Yang Miao(苗扬)^{1,2**}, Xiang Guo(郭祥)¹, Xiao-Jun Zhang(张小军)¹

¹College of Mechanical Engineering and Applied Electronics Technology, Beijing University of Technology, Beijing 100124

²Beijing Key Laboratory of Advanced Manufacturing Technology, Beijing University of Technology, Beijing 100124

(Received 11 December 2019)

To measure the parameters of fiber and to visualize the reshaping process of fiber in air tunnel, an experimental approach is developed in the present work. The tunnel is designed with gradient flow velocity, and the fiber reshaping images as well as the fiber length value are obtained experimentally. An analytical expression of velocity distribution in the tunnel is theoretically derived and the simulated results are obtained. Automatic fiber reshaping including stretch and rotation is verified using the dynamical equation and the multi-spherical chain model. It is shown that pull force by air flow makes a chain of balls become straight and Stokes moment makes the ball chain rotate. Finally, reshaping criterion related with flow velocity is formulated.

PACS: 42.15.Eq, 42.62.-b, 47.10.-g

DOI: 10.1088/0256-307X/37/3/034201

Judgment and measurement of fiber parameters are needed in many application fields. Conventional measurement technology mainly used includes the Bayesian statistic method,^[1] comb-type fiber length analyzer,^[2] roller fiber length test^[3] and almeter.^[4] However, all these measurements must prepare fiber samples from raw materials because fibers are naturally clustered just as cotton ball. In other words, sample fibers need to be taken out from the raw material, their directions should be aligned, and the shape style is stretched. The sample preparations are often complex and time consuming because they are usually adopting mechanical operation. This results in the measurements not being made in real-time or automatically. To realize automatic fiber measurement, we try to make fiber move in air flow to realize fiber shaping and stretching spontaneously instead of mechanical operation. Fiber motion in flow field has attracted attention because of its special characteristics. Researchers have analyzed fiber migration and trajectories in shear flow and in inhomogeneous flow, respectively.^[5,6] Smith and Roberts proposed a model which simplifies the fibers as a chain consisting of spheres and cylinders, and investigated fiber motion in laminar flow.^[7] Bangert and Sagdeo investigated fiber alignment using fluid-dynamic forces.^[8] Yamamoto and Matsuoka proposed special fiber models and simulated fiber fracture and change induced by flow.^[9,10] We investigated high order waves of the fluid and measured fluid slosh using optical technology.^[11,12] In this Letter, we construct an experimental setup, based on the reshaping of a fiber moving in an air tunnel with gradient velocity, to measure fiber length automatically and to visualize reshaping process in real time. We derive an analytical expression of velocity distribution in the air tunnel and obtain the simulated results theoretically. Fiber dynamical equation is established using a multi-spherical chain model and reshaping mechanism of a fiber moving in an incompressible

fluid is discussed. It is shown that the fiber moving in velocity gradient flow could be automatically reshaped, including stretch and rotation. Pull force by air flow makes a ball chain become straight and Stokes moment makes the ball chain rotate. Meanwhile, a criterion formula of fiber reshaping related with flow velocity is achieved. We present both experimental and theoretical results and make a comparison between them. The experimental results and theoretical simulation well agree with each other.

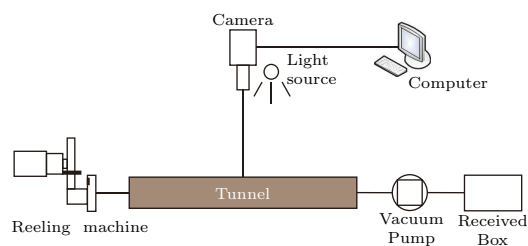


Fig. 1. Schematic diagram of the experimental setup.

The experimental setup shown in Fig. 1 consists of four parts: a reeling machine, an air tunnel, a centrifugal pump and a camera monitoring system. The reeling machine, connecting with air tunnel inlet, takes the separated fibers out from raw materials. The tunnel is made of flexi-glass and its length is 400 mm. The tunnel consists of a cylinder and a cone, and both of them are tight coupling. The cylinder's diameter and length are 20 mm and 200 mm, respectively. The cone length is also 200 mm and its diameters at both ends are 20 mm and 40 mm, respectively. The thickness of the tunnel is 1 mm. The centrifugal pump installed at the tail of the tunnel provides a negative pressure for the tunnel cavity. Therefore, the fibers from the reeling machine are attracted into air tunnel and move in it automatically. The air velocity will increase with the distance in horizontal direction because of the tunnel construction. Meanwhile, the air

*Supported by the National Natural Science Foundation of China under Grant Nos. 51605009 and 51975011.

**Corresponding author. Email: miaoyang@vip.126.com, miaoyang@bjut.edu.cn

© 2020 Chinese Physical Society and IOP Publishing Ltd

velocity decreases in radial direction because of fluid viscosity. The fibers out of the tunnel are received in a box. The negative pressure provided by centrifugal pump is 22500 Pa. The camera (model Basler) is above the tunnel and its distance from the tunnel is 300 mm and its shooting speed is 750 times per second. The camera transmits the captured data transferred into a computer for storing and processing. The processing speed is 5 frames per second.

The experiment was carried many times and the results show that the moving fiber can be reshaped in an air tunnel with gradient velocity distribution. Meanwhile, the fiber length can be measured automatically. Here, two groups of selected experimental results are shown in Fig. 2, in which the fibers are with different shape style at the tunnel inlet. Figure 2(a) shows a fiber just passing the inlet appears crimp. However, it comes straight when the moving distance is near 200 mm, just over the connect nod of cylinder and cone. This result shows the fiber is automatically reshaped during the motion in the tunnel. Figure 2(b) illustrates a fiber near the inlet is straight and still keep this form all the way. Both graphs demonstrate that a fiber moving in this tunnel will become straight finally whether its primary state is crimp or straight. The image this reshaped fiber is captured by the camera processed by the computer. Finally, the fiber length value is arrived. The approach is in real time. We capture two thousand fibers images for a quality cotton and calculate the fiber length. The average length achieved is about 38 mm.

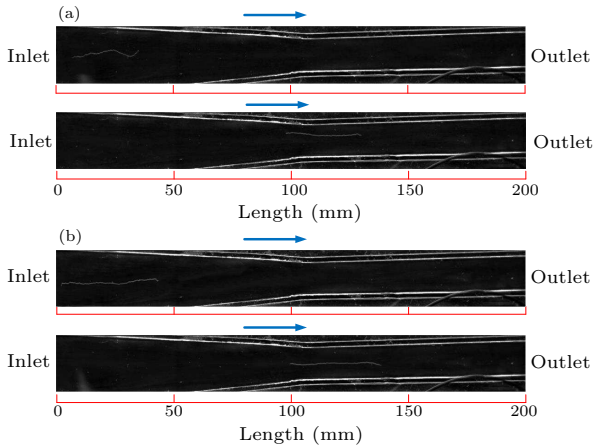


Fig. 2. Shape style variation of fiber moving in air tunnel: (a) crimp to straight, (b) straight all path.

Flow velocity distribution in air tunnel.—It is supposed that the fluid in air tunnel is viscous incompressible and the Navier–Stokes equation is generally used to describe the air dynamical motion. Because the air tunnel structure is just like a cone, the Navier–Stokes equation in cylinder coordinates is expressed as follows:

$$\rho \frac{\partial \mathbf{v}}{\partial t} = \rho g - \frac{dp}{dz} + \mu \left[\frac{1}{r} \frac{\partial}{\partial r} \left(r \frac{\partial \mathbf{v}}{\partial r} \right) \right], \quad (1)$$

where ρ is the air density, \mathbf{v} is the flow velocity, g is

the gravitational acceleration, p is pressure, μ is Newton friction coefficient, r and z (as shown in Fig. 3(a)) are radial and longitudinal coordinates, respectively. When air tunnel runs work stately, it is considered that the velocity distribution is unchanged. This means $\frac{\partial \mathbf{v}}{\partial t} = 0$. The term ρg in Eq. (1) can be neglected because fiber density ρ is small. In this case, Eq. (1), when neglecting high order velocity differential terms, can be simplified to

$$\frac{dp}{dz} = \mu \left[\frac{1}{r} \frac{dv}{dr} \right]. \quad (2)$$

By integrating both sides of Eq. (2), we have the analytical expression of the velocity distribution in the tunnel as follows:

$$v(r) = v_{i0} \left(\frac{r_i}{r_z} \right)^2 \left[1 - \left(\frac{r}{r_z} \right)^2 \right], \quad (3)$$

where $r_z = r_i - \frac{r_i - r_0}{L} z$, $v(r)$ is velocity distribution in the radial coordinate at longitude distance z ; v_{i0} is velocity at the inlet center; r_i , r_0 and r_z are the tunnel radii at inlet, outlet, and distance z , respectively.

Based on Eq. (3), the velocity distribution in the tunnel is plotted in Fig. 3. Figure 3(a) presents the curves at different longitude distances. Figure 3(b) shows the distribution pattern.

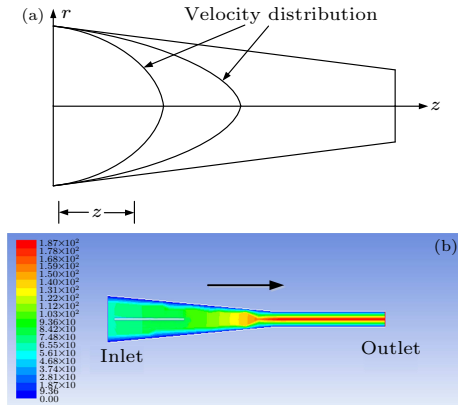


Fig. 3. Velocity distribution in air tunnel: (a) curves, (b) pattern.

Figure 3 shows that the velocity increases with longitude coordinate. Meanwhile, for a given distance z , the velocity decreases with the radial coordinate. This means that the maximum of air speed is at the longitude axis of the tunnel and the air speed increases with moving distance.

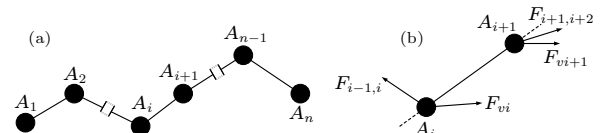


Fig. 4. (a) Diagram of the multi-ball chain model and (b) the force analysis.

Fiber motion equation.—To set up the fiber dynamical equation in air flow, a fiber structure, called the multi-ball chain model, is proposed as Fig. 4(a), in which the fiber is composed of n balls. For simplicity,

the mass of each ball is assumed as the unit. Any adjacent balls are connected by a line with the mass of zero and length of l .

It is assumed that the force between any adjacent balls A_i and A_{i+1} is $F_{i,i+1}$. Then, the dynamical equation of ball A_i is as follows:^[13]

$$\frac{d\mathbf{V}_{bi}}{dt} = F(\mathbf{V}_i - \mathbf{V}_{b,i}) - \mathbf{F}_{i-1,i} + \mathbf{F}_{i,i+1} - \left(1 - \frac{\rho}{\rho_p}\right)g\mathbf{k},$$

$$i = 1, 2, \dots, n, \quad (4)$$

where $\mathbf{V}_{b,i}$ is the velocity of ball A_i , \mathbf{V}_i is the air velocity at the surface of the ball. $F = \frac{9\mu_1}{2a^2\rho_b}$, in which a is the radius of ball A_i , μ_1 is the dynamic viscous coefficient between air fluid and fiber surface, t is the time, ρ and ρ_b are the densities of air fluid and fiber, respectively; g is the gravitational acceleration, and \mathbf{k} is unit vector vertical direction; $\frac{1}{F}$ is called the relaxation time of momentum transfer between fluid and fiber. Each term on the right side of Eq. (4) represents the forces acting on ball A_i . The first term is Stokes force \mathbf{F}_{vi} as shown in Fig. 4(b), $\mathbf{F}_{i,i+1}$, $\mathbf{F}_{i-1,i}$ are the stretch forces on ball A_i acted by adjacent balls. The third term is the join forces of gravity and buoyancy which are neglected in Fig. 4(b) because they are much smaller than other forces.^[14] $\mathbf{V}_{b,i} = \frac{d\mathbf{r}}{dt}$, \mathbf{r} is the position coordinate vector of ball A_i .

Using Eq. (4) and subtracting the momentum change rate of ball A_i , one has

$$\frac{d}{dt}(\mathbf{V}_{b,i+1} - \mathbf{V}_{b,i}) = F(\mathbf{V}_{i+1} - \mathbf{V}_i) - F(\mathbf{V}_{b,i+1} - \mathbf{V}_{b,i})$$

$$+ \mathbf{F}_{i-1,i} - 2\mathbf{F}_{i,i+1} + \mathbf{F}_{i+1,i+2}. \quad (5)$$

The left-hand equation can be rewritten as

$$\frac{d}{dt}(\mathbf{V}_{b,i+1} - \mathbf{V}_{b,i}) = \frac{d\boldsymbol{\omega}_i}{dt} \times \mathbf{l}_i + \boldsymbol{\omega}_i \times (\boldsymbol{\omega}_i \times \mathbf{l}_i), \quad (6)$$

where $\boldsymbol{\omega}_i$ is angular velocity vector, \mathbf{l}_i is chain vector between balls A_i and A_{i+1} . It is shown that Eq. (6) is composed of two parts. The first and second terms are related with the chain rotation and the translation motion of the balls A_i and A_{i+1} , respectively.

The flow in the air tunnel could make fiber reshaping including stretch and rotation.

Stretch reshaping.—The air flow in the tunnel will result in the fiber motion and make ball A_{i+1} stretch ball A_i . To analyze the translation motion of the fiber moving in tunnel, we decompose all the terms of Eq. (5) in the direction \mathbf{l}_i (as Fig. (4a)),

$$F(|V_{i+1}| \cos \theta_{i+1,i} - |V_i| \cos \theta_{i,i}) = l_i \omega_i^2 + 2|F_{i,i+1}|$$

$$- |F_{i-1,i}| \cos \phi_{i-1,i} - |F_{i+1,i+2}| \cos \phi_{i+1,i}, \quad (7)$$

where $\theta_{i+1,i}$, $\theta_{i,i}$, $\theta_{\omega i}$, $\phi_{i-1,i}$, and $\phi_{i+1,i}$ are the angles between vectors \mathbf{V}_{i+1} , \mathbf{V}_i , $\boldsymbol{\omega}_i$, $\mathbf{F}_{i-1,i}$, $\mathbf{F}_{i+1,i+2}$ and vector \mathbf{l}_i , respectively.

If $|F_{i-1,i}| = |F_{i,i+1}| = |F_{i+1,i+2}|$, then $2|F_{i,i+1}| - |F_{i-1,i}| \cos \phi_{i-1,i} + |F_{i+1,i+2}| \cos \phi_{i+1,i} = |F_{i,i+1}|(2 - \cos \phi_{i-1,i} - \cos \phi_{i+1,i}) > 0$.

By substituting the above inequality into Eq. (7) yields

$$F(|V_{i+1}| \cos \theta_{i+1,i} - |V_i| \cos \theta_{i,i}) > l_i \omega_i^2 \sin \theta_{\omega i}. \quad (8)$$

If the velocity of air flow in tunnel satisfies this equation, then ball A_{i+1} will stretch ball A_i completely during the all moving period. Because the air flow is nearly laminar, we have $\cos \theta_{i+1,i} \approx \cos \theta_{i,i} \approx 0$. Meanwhile, the $|V_{i+1}|$ is greater than $|V_i|$ because air flow of the tunnel used in experiment has velocity gradient. Fiber angular velocity is almost zero in the primary because the rotation does not occur at the beginning. These show that our tunnel meets the requirement of Eq. (8) and the fiber moving in it is certainly stretched.

Rotation reshaping.—If the chain of balls A_i and A_{i+1} is not parallel to the tunnel axis, the air flow will make the fiber rotate. In order to analyze the rotation of the fiber moving in tunnel, we decompose all the terms of Eq. (5) in the direction perpendicular to \mathbf{l}_i in rotation plan (as Fig. (4b)),

$$l_i \frac{d\omega_i}{dt} = F(|V_{i+1}| \sin \theta_{i+1,i} - |V_i| \sin \theta_{i,i})$$

$$+ |F_{i-1,i}| \sin \phi_{i-1,i} + |F_{i+1,i+2}| \sin \phi_{i+1,i}. \quad (9)$$

If $|F_{i-1,i}| = |F_{i,i+1}| = |F_{i+1,i+2}|$ and we multiply l_i on both the sides of the above equation, we have

$$l_i^2 \frac{d\omega_i}{dt} = Fl_i(|V_{i+1}| \sin \theta_{i+1,i} - |V_i| \sin \theta_{i,i})$$

$$+ |F_{i,i+1}| l_i (\sin \phi_{i+1,i} + \sin \phi_{i-1,i}). \quad (10)$$

Suppose that the values of $\theta_{i+1,i}$ and $\theta_{i,i}$ are all positive, $\phi_{i-1,i}$ and $\phi_{i+1,i}$ are positive in clockwise and negative in anticlockwise. Equation (10) could be explained physically such that the left side is the product of the rotational inertia l_i^2 and the angular acceleration $\frac{d\omega_i}{dt}$, $Fl_i(|V_{i+1}| \sin \theta_{i+1,i} - |V_i| \sin \theta_{i,i})$ is Stokes force moment, and $|F_{i,i+1}| l_i (\sin \phi_{i+1,i} + \sin \phi_{i-1,i})$ is the join force moment of the adjacent balls. Because $|V_{i+1}| > |V_i|$ and the air flow is nearly laminar, we have

$$Fl_i(|V_{i+1}| \sin \theta_{i+1,i} - |V_i| \sin \theta_{i,i}) \geq 0. \quad (11)$$

If the chain of balls A_i and A_{i+1} is parallel to the direction of the air flow, then both sides of Eq. (11) are identical and the value of Stokes force moment is zero. However, if the angle between the velocity and the ball chain is nonzero, the air flow has to produce Stokes force moment which changes the fiber rotation state. The rotation tends to decreasing the angle value. Lastly, the angle between the velocity and the ball chain tends to zero. This means that the fiber direction is parallel to the longitude axis of the tunnel. Such a rotation in the tunnel with gradient velocity is called the rotation reshaping.

In summary, fiber length automatic measurement and reshaping processes visualized in real time are proposed and realized. Experiments show that a fiber moving in the air tunnel with gradient velocity can be

reshaped to become straight. An analytical expression of velocity distribution in the tunnel is theoretically derived. The simulated results show that the tunnel has a velocity gradient in both longitude and radial directions, and the maximal velocity locates at the tunnel axis. The dynamic equation of the fiber using a multi-spherical chain model is established. It is verified that a fiber moving in a tunnel can be automatically reshaped, including stretch and rotation. The reshaping criteria are achieved for stretch and rotation.

References

- [1] Goris S, Back T, Yanev A, Brands D, Drummer D and Osswald T A 2018 *Polym. Compos.* **39** 4058
- [2] Goris S and Osswald T A 2017 *Polym.-Plast. Technol. Eng.* **73** 46
- [3] Cai Y, Cui X, Rodgers J, Thibodeaux D, Martin V, Watson M and Pang S S 2013 *Text. Res. J.* **83** 961
- [4] Majumdar A, Ciocoiu M and Blaga M 2008 *Fibers Polym.* **9** 210
- [5] Perumal V, Gupta R K, Bhattacharya S N and Costa F S 2019 *Polym. Compos.* **40** 3573
- [6] Feldman L 1996 *Text. Res. J.* **36** 809
- [7] Smith A C and Roberts W W 1994 *Text. Res. J.* **64** 335
- [8] Bangert L H and Sagdeo P M 1977 *Text. Res. J.* **47** 773
- [9] Yamamoto S and Matsuoka T 1995 *Polym. Eng. Sci.* **35** 1022
- [10] Yamamoto S and Matsuoka T 1994 *J. Chem. Phys.* **100** 3317
- [11] Miao Y and Wang S 2014 *Opt. Commun.* **315** 91
- [12] Miao Y, Wu C, Wang N and You J Q 2016 *Chin. Phys. Lett.* **33** 074206
- [13] Sun Z, Kang X Q and Wang X H 2005 *Mater. & Des.* **26** 59
- [14] Dhanasekaran J and Koch D L 2019 *J. Fluid Mech.* **879** 121